# CoMFA analyses of C-2 position Salvinorin A analogs at the kappa-opioid receptor provides insights into epimer selectivity

Donna L. McGovern [a], Philip D. Mosier [a], Bryan L. Roth [b], Richard B. Westkaemper [a,*]

[a] Department of Medicinal Chemistry, P.O. Box 980540, School of Pharmacy, Virginia Commonwealth University, Richmond, VA 23298-0540, United States
[b] Department of Pharmacology, University of North Carolina School of Medicine, Chapel Hill, NC 27599, United States

ABSTRACT

The highly potent and kappa-opioid (KOP) receptor-selective hallucinogen Salvinorin A and selected analogs have been analyzed using the 3D quantitative structure–affinity relationship technique Comparative Molecular Field Analysis (CoMFA) in an effort to derive a statistically significant and predictive model of salvinorin affinity at the KOP receptor and to provide additional statistical support for the validity of previously proposed structure-based interaction models. Two CoMFA models of Salvinorin A analogs substituted at the C-2 position are presented. Separate models were developed based on the radioligand used in the kappa-opioid binding assay, [$^3$H]diprenorphine or [$^{125}$I]6$\beta$-iodo-3,14-dihydroxy-17-cyclopropylmethyl-4,5$\alpha$-epoxymorphinan ([$^{125}$I]IOXY). For each dataset, three methods of alignment were employed: a receptor-docked alignment derived from the structure-based docking algorithm GOLD, another from the ligand-based alignment algorithm FlexS, and a rigid realignment of the poses from the receptor-docked alignment. The receptor-docked alignment produced statistically superior results compared to either the FlexS alignment or the realignment in both datasets. The [$^{125}$I]IOXY set (Model 1) and [$^3$H]diprenorphine set (Model 2) gave $q^2$ values of 0.592 and 0.620, respectively, using the receptor-docked alignment, and both models produced similar CoMFA contour maps that reflected the stereoelectronic features of the receptor model from which they were derived. Each model gave significantly predictive CoMFA statistics (Model 1 PSET $r^2$ = 0.833; Model 2 PSET $r^2$ = 0.813). Based on the CoMFA contour maps, a binding mode was proposed for amine-containing Salvinorin A analogs that provides a rationale for the observation that the $\beta$-epimers ($R$-configuration) of protonated amines at the C-2 position have a higher affinity than the corresponding $\alpha$-epimers ($S$-configuration).

© 2010 Published by Elsevier Inc.

## 1. Introduction

Salvinorin A (Fig. 1) is a highly potent and selective kappa-opioid (KOP) receptor agonist and the most potent naturally occurring hallucinogen known [1]. The terpenoid was first isolated from the plant Salvia divinorum and characterized by Ortega [2] in 1982. The same compound was later isolated from S. divinorum by Valdes [3] in 1984 who reported its psychoactive properties in mice. S. divinorum has been used for centuries by the Mazatec Indians of Mexico for divination and is indigenous to a small area in the Sierra Mazateca Mountains. The plant was subsequently propagated and can now be found growing in widespread locations, sold by nurseries, and sold through the Internet for its hallucinogenic properties as both dried leaves and fortified plant extracts. The FDA has yet to schedule Salvinorin A, its extracts, or dried leaves as a controlled substance, although many countries and several states within the United States have adopted legislation banning the use of S. divinorum and related products.

Since the discovery that Salvinorin A is a remarkably potent and selective KOP receptor agonist [1], a large number of analogs have been synthesized, especially C-2 position analogs [4–19]. A smaller number of C-4 position analogs [4,5,7,19–21] and analogs with alterations of the furan ring [15,22,23] have also been reported in the literature. By inspection, the data suggest that very little change is tolerated at the C-4 position or the furan ring. Thus, attention was focused on C-2 modified structures for which a wide range of affinities have been reported.

Salvinorin A is unique among hallucinogens in that its chemical structure lacks a basic amine group. This is significant because such a moiety was previously thought to be required for high ligand affinity at aminergic and other closely related G Protein-Coupled Receptors (GPCRs). It is generally understood that the receptor-ligand interaction involving the amine is mediated by a conserved aspartate residue (D$^{3.32}$) on transmembrane helix 3 (TM3) through formation of a hydrogen-bonded salt bridge, anchoring the ligand in the binding site. Thus it is quite surprising that Salvinorin A's
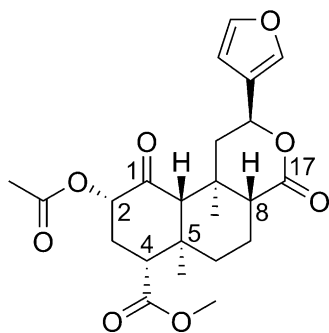
Fig. 1. Salvinorin A (**1**).

high affinity for the KOP receptor is comparable to that of amine-containing ligands [24].

The molecular mechanisms by which Salvinorin A achieves its exquisite affinity and selectivity for the KOP receptor is an active and ongoing area of research. Our working hypothesis is that by removing the amine from a ligand, its affinity for the many aminergic and related receptors decreases dramatically, resulting in high selectivity. That is, without the amine "anchor", the receptor becomes more sensitive to changes in the ligand structure, and therefore the stereoelectronic nature of the ligand and its complementarity to the target receptor become much more important factors in determining the affinity of the ligand for the receptor.

Although the affinity of hundreds of Salvinorin A analogs for the KOP receptor has been reported, there is very little published information regarding the QSAR of these compounds. In 2006, Singh et al. [25] described a quantitative and predictive structure–affinity model derived using a KOP receptor homology model and virtual screening techniques with a set of a set of 27 Salvinorin A analogs with modifications at the C-1, C-2, C-4 and C-17 positions. In the same year, Pandit et al. [26] reported a CoMFA model for C-2 position Salvinorin A analogs, though the details of this study have yet to be published.

Comparative Molecular Field Analysis (CoMFA), a three-dimensional quantitative structure–activity relationship (3D-QSAR) methodology, may be used to rationalize and predict ligand–receptor interactions when used in conjunction with homology modeling. In CoMFA, a 3D-QSAR model is constructed by correlating regions of steric and electrostatic fields with experimentally obtained affinity data for a set of aligned ligands (the training set or TSET). Information contained in the model can then be used for the design and prediction of binding affinities of new ligands (the prediction set or PSET) for the target receptor. The resulting models are critically dependent on the ligand alignment method used. If receptor structure-based ligand docking is used to generate the alignment, statistical 3D-QSAR methods like CoMFA may be used to complement and provide additional statistical support for the proposed ligand binding modes. Salvinorin A analogs are well-suited for a CoMFA study because the core of the molecule does not vary and it is conformationally constrained due to its polycyclic structure, much like the steroid system presented in the initial description of the method [27].

We report here our successful generation of statistically significant and predictive CoMFA models describing the interaction of C-2 Salvinorin A analogs with the KOP receptor and our use of these models to propose a binding mode for C-2 amine-containing Salvinorin A analogs.

## 2. Experimental methods

### 2.1. Receptor and ligand structures

CoMFA studies were performed using SYBYL software (version 7.3, Tripos Associates, St. Louis, MO) on an HP xw9400 workstation running Red Hat Enterprise Linux 4. The human KOP receptor model used here was built based on the coordinates of activated bovine rhodopsin crystal as previously described [24,28,29]. Compounds were constructed using the crystal structure [2] of Salvinorin A, (Cambridge Structural Database code = BUJJIZ) as the template and then energy-minimized using the Tripos Force Field (Gasteiger-Hückel charges; distance-dependent dielectric constant = 4.0; default parameters elsewhere).

### 2.2. Ligand docking and alignment

To explore the effect of ligand superimposition on the resulting statistical models, three methods of alignment were employed in each study. In the first, the automated docking routine GOLD was used to produce an alignment based on docked solutions of ligands to a previously described model [24,28,29] of the KOP receptor. Thus, the ligand ensemble is that produced by docking with no explicit ligand-ligand atom superposition performed. The second, a ligand-based method, was obtained using FlexS [30]. The third alignment method was a rigid realignment of the receptor-docked alignment.

Docking of salvinorin compounds was performed using GOLD (version 4.0, Cambridge Crystallographic Data Center, Cambridge, UK) as previously described [24,28,29]. Ten docking runs were performed for each compound in the dataset. The initial alignment was generated by selecting the docked solution in which (a) a furan oxygen-Q115$^{2.60}$ H-bond was present and (b) the stereochemical interactions appeared most reasonable for each ligand. In most cases the chosen pose was the top-ranked solution. This resulted in an alignment that resembled the previously postulated model of Salvinorin A in the KOP receptor [24,28,29] (Fig. 2). The second alignment method (using the same dataset) was performed with FlexS (version 1.20.3, BioSolveIT GmbH, Sankt Augustin, Germany). FlexS aligns the conformation and orientation of a ligand molecule relative to a reference molecule (template) that is treated as rigid. The molecule to be superimposed is partitioned into fragments. An 'anchor fragment' is placed first and the remaining fragments are added iteratively, allowing conformational flexibility at each step [30]. Compound **4** was used as the template for this alignment because it is the longest C-2 chain that still retains high affinity. The third alignment method, a realignment of the docked poses in the receptor-docked alignment, was performed by aligning all compounds to Salvinorin A using the SYBYL fit-atoms method. Carbon atoms C-2, C-4 and C-5 of Salvinorin A and the analogous atoms of each analog were selected for the fitting process.

### 2.3. Dataset generation

The quality and nature of the data used to construct the CoMFA model is of prime importance in obtaining an accurate, predictive model. Binding affinity data can vary from lab to lab depending on the assay methods, radioligand and cell lines employed. The choice of radiolabeled ligand can dramatically affect the values obtained [31,32], as can the level of gene expression that results in differing receptor densities in cloned cell lines [33]. Therefore pooling of data for a CoMFA study is generally discouraged. In this work, two independent CoMFA studies were undertaken, one in which [$^{125}$I]IOXY (6β-iodo-3,14-dihydroxy-17-cyclopropylmethyl-4,5α-epoxymorphinan) was used as the assay radioligand and a second in which [$^3$H]diprenorphine was the assay radioligand.

Compounds that are protonated at physiological pH (e.g. amines) and compounds with $K_i > 1,000$ nM were not included in the dataset. Protonated compounds would, perhaps, form an ion-pair interaction with D138$^{3.32}$ (Ballesteros-Weinstein numbering system [34,35]) of transmembrane helix 3 (TM3) or E209$^{xl2.49}$ of the extracellular loop 2 (EL2) that may result in a significant difference in the binding mode compared to that of
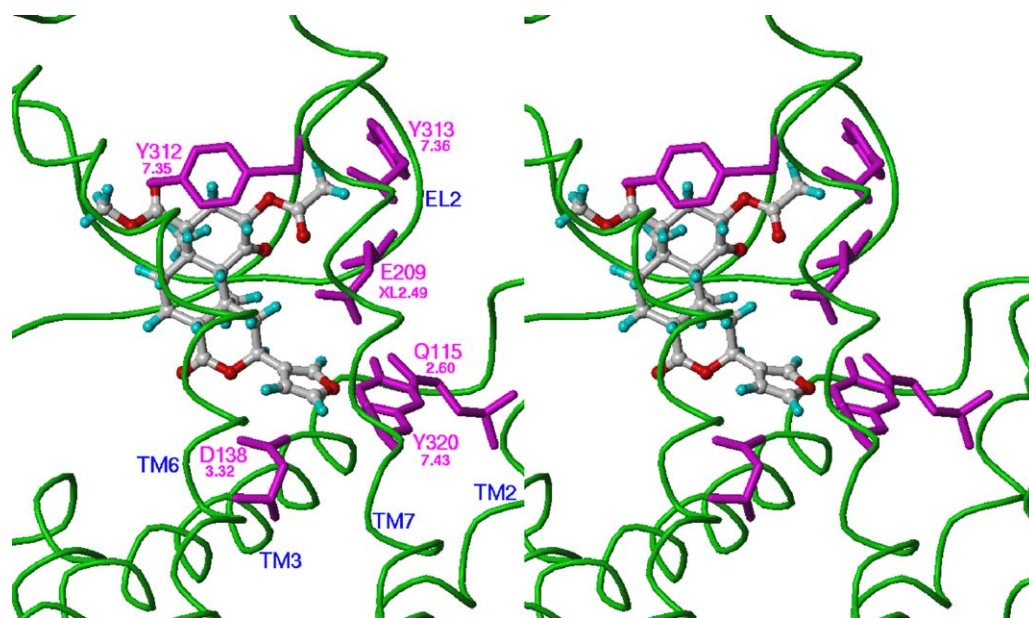
**Fig. 2.** Stereo view of Salvinorin A docked in the KOP receptor. Salvinorin A is shown in ball and stick and colored according to atom type. Residues are colored magenta.

Salvinorin A. MOPAC charges (AM1) were then applied to each aligned dataset before initiating the CoMFA analyses. Training set compounds were chosen randomly with the only criterion being that they cover a wide range of $K_i$ values.

### 2.4. CoMFA model generation

In the 3D-QSAR analysis, all aligned training set (TSET) molecules are placed in a cubic lattice (grid) that is divided into hundreds (or thousands) of points at a regular spacing. In this CoMFA study, the default grid spacing of 2.0 Å was used. Lennard–Jones 6-12 and Coulomb potentials were used to calculate the steric and electrostatic interaction fields, respectively. An sp$^3$-hybridized carbon atom with a charge of +1 was used as the probe atom. The standard default settings were used, except for the steric and electrostatic cutoff values that were each varied by increments of 5 kcal/mol from 10 to 50 kcal/mol in order to obtain the highest value of $q^2$ for each dataset alignment. All $K_i$ data were converted to p$K_i$ ($-\log K_i$). The p$K_i$ represents the dependent variable while the CoMFA field potentials at each grid point represent the independent variables in the partial least squares (PLS) regression analyses. The standard "leave-one-out" (LOO) cross-validation method was used to obtain the predictive correlation coefficient $q^2$ and the optimal number of principal components (PCs). In the LOO method, each compound is excluded one at a time. A model is then constructed from the remaining compounds to predict the activity of the excluded compound. The optimal number of PCs chosen corresponds to the smallest error of prediction and the highest $q^2$. The PLS analysis was then repeated with no validation using the optimal number of PCs to generate the CoMFA model. The $r^2$ statistic, which is a measure of the amount of variation in the dependent variable that can be ascribed to variation in the independent variable, and the standard error of estimate (SEE) were obtained from this model. The $r^2_{\text{pred}}$ was obtained from the linear regression of the experimental vs. predicted p$K_i$ values of the prediction set (PSET). A column filter of 3 or 4 kcal/mol was applied to improve efficiency and reduce noise in the field data. The filter procedure excludes those columns whose grid point potentials vary below the set cutoff. In the first model, region focusing [36] was used to improve the model statistics. Region focusing divides the lattice grid into multiple grids with smaller lattice spacing and

then performs a CoMFA analysis on each grid. Grids below a determined $q^2$ cutoff are eliminated and another CoMFA analysis is performed on the remaining grids as a whole resulting in enhancement of those lattice points and, in some cases, an improved statistical outcome.

## 3. Results and discussion

### 3.1. Salvinorin A–KOP receptor interaction model

Salvinorin A consists of a rigid hydrophobic core that contains eight hydrogen-bond accepting oxygen atoms. In the postulated model of Salvinorin A docked in the human KOP receptor as recently described [24] (Fig. 2), the oxygen of the furan ring may form a hydrogen bond with both Q115$^{2.60}$ and Y320$^{7.43}$. A hydrogen bond interaction with these two residues is supported by site-directed mutagenesis studies [24,29,37] in which KOP receptor mutants Q115A, Y320A and Y320F all showed a substantial decrease in the binding affinity of Salvinorin A as compared to wild type KOP receptor. An additional hydrogen bond may possibly exist between Y312$^{7.35}$ and the methoxy oxygen of the C-4 position methyl ester, although the KOP receptor mutants Y312A and Y312F showed only a modest decrease [29,37] in the binding affinity of Salvinorin A (4.5-fold decrease for the KOP receptor Y312A mutant [37]). In addition, there is a likely hydrophobic interaction between Y313$^{7.36}$ and the methyl group of the C-2 position acetoxy moiety of Salvinorin A that is supported by site-directed mutagenesis studies [29,37] in which there are substantial losses of affinity for the KOP receptor Y313A mutant but little or no loss for the Y313F mutant (indicating a hydrophobic interaction rather than a hydrogen bond interaction). Chimeric receptor studies [28,37,38] also highlight the importance of residues in TM2 and TM7 in the binding of Salvinorin A to the KOP receptor. In addition, substituted cysteine accessibility method (SCAM) studies [24,28,29] indicate that these residues are accessible in the binding pocket. Finally, the putative Salvinorin A binding mode is consistent with recently reported affinity labeling experiments that indicate that the C-2 substituent in near TM7 [39].

It is perhaps useful to compare the KOP receptor receptor homology model employed here with that of the more recently determined β$_2$-adrenoceptor crystal structure. Although the KOP receptor model was based on activated bovine rhodopsin as a

template (PDB ID = 2I37) [40], several modifications were applied during the course of model refinement. The two most notable of these in terms of the conformation of the KOP receptor binding site are briefly described here. First, extracellular loop 2 (EL2) was repositioned using molecular dynamics to a location nearer to the extracellular opening of the receptor [29], enlarging the binding site cavity. Although it has been suggested that the EL2 loop be removed for purposes of ligand docking [41], there is evidence that EL2 may in fact interact with Salvinorin A [24]. Second, the extracellular portion of TM2 was rotated [28] to bring the model in line with mutagenesis data that suggests that, along with other mutations, Q115$^{2.60}$ may interact with Salvinorin A [37,38]. As a result, the conformation of the refined KOP receptor model differs as much compared to the original template as to the $\beta_2$-adrenoceptor (PDB ID = 2RH1), consistent with the suggestion that homology models of the opioid receptors would be among those that would benefit most from the determination of the structure of a GPCR not closely related to those currently available [42].

### 3.2. Alignment methods

One can make the assumption that the salvinorin analogs would bind in the same way as Salvinorin A since the core of the molecule, in most cases, remains identical. If this is the case, then methods such as FlexS or an atom-to-atom fit that result in a "tight" alignment of molecules (low RMSD values for those atoms in the common core structure) might be expected to result in a good CoMFA model. However, it was found that the receptor-docked alignment, in which many of the molecules' docked position and/or orientation deviated from Salvinorin A (some by as

much as 4.5 Å), was found to be superior to FlexS and the realignment. In fact, in previous work (data not shown), several alignment methods available in the SYBYL package were evaluated including manual atom fitting, database alignment, GALAHAD and Surflex-Sim that resulted in well-aligned molecules but gave poor CoMFA statistics. Salvinorin A analogs may thus bind in a similar, but non-identical manner to the parent. Accordingly, a receptor-docked alignment may provide a better picture for predictive purposes, since the noted variability in the position of the rigid core represents the receptor's ability to recognize and accommodate (up to a point) ligand analogs with sidechains of varying size.

A rigid realignment of the docked poses was performed in order to evaluate which type of alignment is more predictive: the alignment based on the receptor's perspective (the receptor-docked alignment) or one based on the ligand's perspective (the realignment) [43]. This realignment resulted in the core of the molecules being very well aligned but exhibited the poorest CoMFA statistics of the three types of alignments: FlexS, receptor-docked or realigned (results not shown).

### 3.3. CoMFA results for the [$^{125}$I]IOXY dataset

The [$^{125}$I]IOXY dataset consisted of 34 Salvinorin A analogs in which [$^{125}$I]IOXY was used as the assay radioligand for the determination of affinity (Table 1). This dataset was divided into a TSET of 23 compounds and a PSET of 11 compounds. The three alignments employed are shown in Fig. S1. Although the use of FlexS results in a "tighter" alignment of the molecules (i.e. lower RMSD for the scaffold atoms), this alignment gave statistically poorer results ($q^2 = 0.311$) as compared to the model based on the receptor-docked alignment (Model 1; region-focused $q^2 = 0.592$) for the identical

**Table 1**
Model 1 dataset of 34 compounds using [$^{125}$I]IOXY as the assay radioligand.
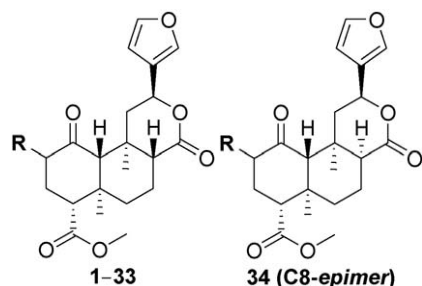


| Compound | R | $K_i$ (nM) | Ref. | Set[b] | exp. | −RF | −RF resi. | +RF | +RF resi. |
|---|---|---|---|---|---|---|---|---|---|
| **1** | | 1.9 | [17] | T | 8.72 | 8.66 | 0.06 | 8.71 | 0.01 |
| **2** | | 280 | [17] | T | 6.55 | 6.41 | 0.14 | 6.42 | 0.13 |
| **3** | | 1.8 | [18] | T | 8.74 | 8.58 | 0.16 | 8.61 | 0.14 |
| **4** | | 4 | [18] | T | 8.40 | 8.39 | 0.01 | 8.39 | 0.01 |
| **5** | | 15 | [18] | P | 7.82 | 7.99 | −0.17 | 8.06 | −0.24 |

The header for the $pK_i$[a] columns spans: Set[b], exp., −RF, −RF resi., +RF, +RF resi.

**Table 1** (*Continued*)
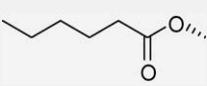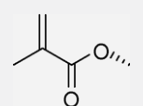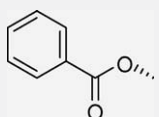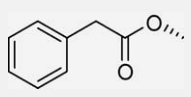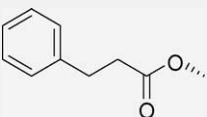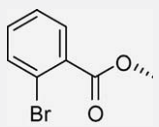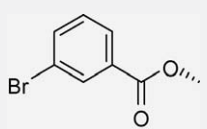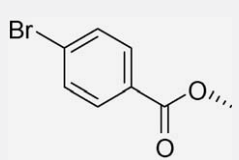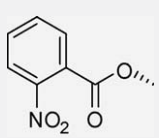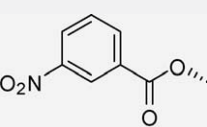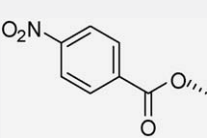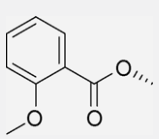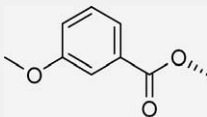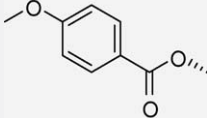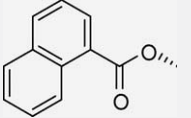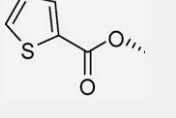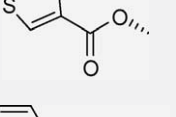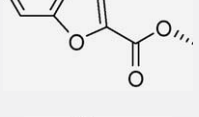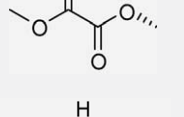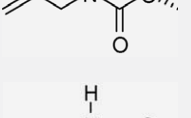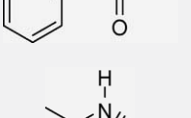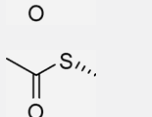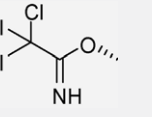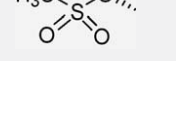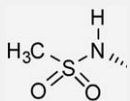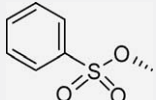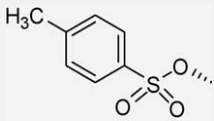
| Compound | R | $K_i$ (nM) | Ref. | Set[b] | exp. | −RF | −RF resi. | +RF | +RF resi. |
|---|---|---|---|---|---|---|---|---|---|
| 6 | | 70 | [18] | T | 7.15 | 7.18 | −0.03 | 7.18 | −0.03 |
| 7 | | 42 | [11] | T | 7.38 | 7.44 | −0.06 | 7.45 | −0.07 |
| 8 | | 90 | [17] | T | 7.05 | 7.00 | 0.05 | 6.99 | 0.06 |
| 9 | | 290 | [18] | P | 6.54 | 6.29 | 0.25 | 6.22 | 0.34 |
| 10 | | 180 | [18] | P | 6.74 | 6.88 | −0.14 | 6.96 | −0.22 |
| 11 | | 90 | [17] | T | 7.05 | 7.11 | −0.05 | 7.14 | −0.09 |
| 12 | | 70 | [17] | P | 7.15 | 6.73 | 0.42 | 6.79 | 0.36 |
| 13 | | 740 | [17] | T | 6.13 | 6.04 | 0.09 | 6.10 | 0.03 |
| 14 | | 900 | [17] | T | 6.05 | 6.09 | −0.04 | 6.10 | −0.05 |
| 15 | | 800 | [17] | P | 6.10 | 6.53 | −0.43 | 6.51 | −0.41 |
| 16 | | 570 | [17] | P | 6.24 | 5.90 | 0.34 | 6.01 | 0.23 |
| 17 | | 230 | [17] | T | 6.64 | 6.61 | 0.03 | 6.59 | 0.05 |

The $pK_i$[a] header spans the Set[b], exp., −RF, −RF resi., +RF, and +RF resi. columns.

**Table 1** (*Continued*)

| Compound | R | $K_i$ (nM) | Ref. | p$K_i$[a] | | | | | |
|---|---|---|---|---|---|---|---|---|---|
| | | | | Set[b] | exp. | −RF | −RF resi. | +RF | +RF resi. |
| **18** |  | 550 | [17] | P | 6.26 | 6.31 | −0.05 | 6.24 | 0.02 |
| **19** |  | 540 | [17] | T | 6.27 | 6.26 | 0.01 | 6.31 | −0.04 |
| **20** |  | 410 | [17] | T | 6.39 | 6.42 | −0.03 | 6.37 | 0.02 |
| **21** |  | 260 | [17] | T | 6.59 | 6.63 | −0.04 | 6.58 | 0.01 |
| **22** |  | 80 | [17] | P | 7.10 | 7.18 | −0.08 | 7.34 | −0.24 |
| **23** |  | 70 | [17] | T | 7.15 | 7.10 | 0.05 | 7.13 | 0.02 |
| **24** |  | 430 | [11] | P | 6.37 | 6.34 | 0.03 | 6.50 | −0.13 |
| **25** |  | 120 | [11] | T | 6.92 | 6.95 | −0.03 | 6.95 | −0.03 |
| **26** |  | 93 | [11] | P | 7.03 | 7.21 | −0.18 | 7.26 | −0.23 |
| **27** |  | 30 | [17] | T | 7.52 | 7.86 | −0.34 | 7.54 | −0.02 |
| **28** |  | 5.7 | [17] | P | 8.24 | 7.86 | 0.38 | 7.88 | 0.36 |
| **29** |  | 64 | [11] | T | 7.19 | 7.19 | 0.00 | 7.21 | −0.02 |
| **30** |  | 2.3 | [11] | T | 8.64 | 8.74 | −0.10 | 8.73 | −0.09 |

**Table 1** (Continued )

| Compound | R | $K_i$ (nM) | Ref. | $pK_i$[a] | | | | | |
|---|---|---|---|---|---|---|---|---|---|
| | | | | Set[b] | exp. | −RF | −RF resi. | +RF | +RF resi. |
| **31** | | 260 | [17] | T | 6.59 | 6.69 | −0.10 | 6.62 | −0.03 |
| **32** | | 60 | [18] | T | 7.22 | 7.34 | −0.12 | 7.26 | −0.04 |
| **33** | | 50 | [18] | T | 7.30 | 7.30 | 0.00 | 7.28 | 0.02 |
| **34** | | 38 | [11] | T | 7.42 | 7.34 | 0.08 | 7.37 | 0.05 |

[a] exp.: experimentally determined value; –RF: predicted value without region focusing; –RF resi.: residual (experimental value – predicted value) without region focusing; +RF: predicted value with region focusing; +RF resi.: residual with region focusing.
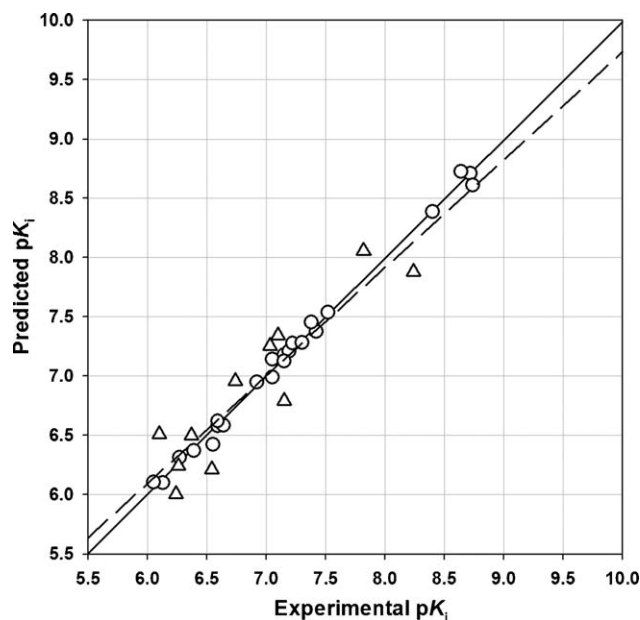[b] T: training set, P: prediction set.

training sets. Region focusing did not improve the FlexS model statistics in this case. The realigned set of molecules, exhibiting the 'tightest' fit, resulted in a $q^2 = 0.526$ after region focusing but a poor $r^2 = 0.767$. Predicted $pK_i$ values were also poor for the FlexS alignment and realignment resulting in 6 of the 34 compounds in the FlexS set and 8 of the 34 compounds in the realigned set having a residual value (experimental $pK_i$ – predicted $pK_i$) greater than the desired range of $\pm 0.50$ $pK_i$ units (results not shown), whereas all values fell within the desired range for the receptor-docked alignment (Table 1). It is hypothesized that the receptor-docked alignment paints a "truer" picture of how ligands might bind to the receptor site, resulting in a more accurate CoMFA contour map reflecting the residues surrounding the molecule in its docked position.

Model 1 CoMFA statistics (receptor-docked alignment) are shown in Table 2. A statistically significant ($F = 465$) and predictive ($q^2 = 0.592$) model was obtained after region focusing, indicating the robustness of the model. The model was shown to have predictive power (PSET $r^2 = 0.833$) and that the slopes of the TSET and PSET regression lines were both close to the ideal value of 1.0. The linear regression plots for Model 1 training and predicted datasets are shown in Fig. 3. The region-focused CoMFA contour maps are shown in Fig. 4.

**Table 2**
CoMFA statistics for Models 1 and 2..

| Parameter | Model 1 | | Model 2 |
|---|---|---|---|
| | Initial value | Region-focused value | Initial value |
| Number of Compounds (TSET) | 23 | 23 | 34 |
| Steric cutoff (kcal/mol) | 25.0 | 25.0 | 35.0 |
| Electrostatic cutoff (kcal/mol) | 35.0 | 35.0 | 30.0 |
| Column filtering (kcal/mol) | 3.0 | 4.0 | 3.0 |
| Number of components | 6 | 6 | 6 |
| Cross-validated $r^2$ ($q^2$) | 0.491 | 0.592 | 0.620 |
| Correlation coefficient $r^2$ (TSET) | 0.991 | 0.994 | 0.989 |
| Standard error of the estimate (SEE) | 0.090 | 0.071 | 0.107 |
| F statistic | 283 | 465 | 395 |
| Steric contribution (%) | 34.3 | 39.3 | 35.4 |
| Electrostatic contribution (%) | 65.7 | 60.7 | 64.6 |
| Number of Compounds (PSET) | 11 | 11 | 13 |
| Correlation coefficient $r^2$ (PSET) | 0.841 | 0.833 | 0.813 |

A region of bulk tolerance (green) can be seen around the C-2 position (Fig. 4a) extending approximately three carbons in length from the carbonyl carbon. The binding affinity data indicates that affinity decreases sharply for esters with chain lengths larger than four carbons in length at the C-2 position. This bulk tolerance region falls within a hydrophobic pocket formed from Y312[7.35], Y313[7.36] and I316[7.39]; this pocket would not be expected to accommodate long chain lengths of greater than four carbons. A region of bulk intolerance (yellow) can be seen behind the C-1 position and in the receptor; this is the region occupied by extracellular loop 2 (EL2) near the disulfide bridge linking the EL2 with transmembrane helix 3 (TM3). In the electrostatic contour map (Fig. 4b) several areas where electronegativity enhances affinity (red) are positioned around the ester and carbonyl oxygens of the molecule. A small area in which electropositive atoms on the



**Fig. 3.** Model 1 linear regression plots. Open circles with a solid regression line indicate the training set and open triangles with a dashed regression line refer to the prediction set.
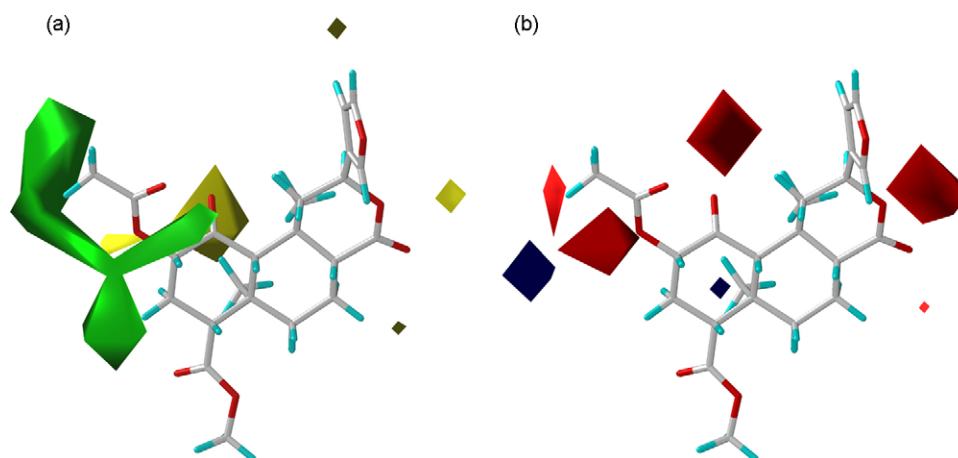
**Fig. 4.** Model 1 CoMFA contour maps. (a) Green and yellow contours show regions of steric tolerance and intolerance, respectively. (b) Red and blue contours show regions where negative and positive electrostatic potential, respectively, are favored.

ligand enhance affinity (blue) can be seen on the β (above the plane of the paper) side of the C-2 position ester group. In the receptor, this blue region is found to fall near the negatively charged carboxylate moiety of E297[6.58] on TM6.

### 3.4. CoMFA results for the [³H]diprenorphine dataset

The [³H]diprenorphine dataset consisted of 47 compounds in which [³H]diprenorphine was used as the assay radioligand

**Table 3**
Model 2 dataset using [³H]diprenorphine as the assay radioligand.
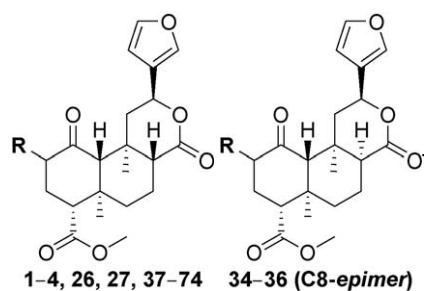


| Compound | R | $K_i$ (nM) | Ref. | Set[a] | $pK_i$[b] exp. | pred. | resi. |
|---|---|---|---|---|---|---|---|
| **1** | | 2.4 | [14] | T | 8.62 | 8.40 | 0.22 |
| **2** | | 155 | [7] | T | 6.81 | 6.71 | 0.10 |
| **3** | | 7.2 | [7] | T | 8.14 | 8.14 | 0.00 |
| **4** | | 4.9 | [7] | P | 8.31 | 7.81 | 0.50 |
| **26** | | 282 | [4] | P | 6.55 | 6.89 | -0.34 |
| **27** | | 149 | [7] | T | 6.83 | 6.97 | -0.14 |

**Table 3** (*Continued*)
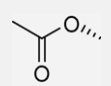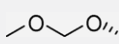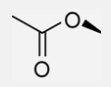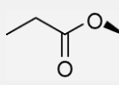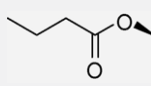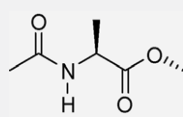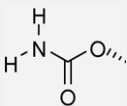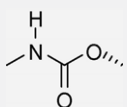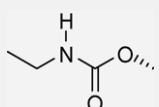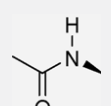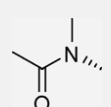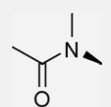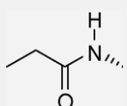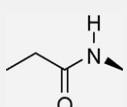
| Compound | R | $K_i$ (nM) | Ref. | Set[a] | $pK_i$[b] | | |
|---|---|---|---|---|---|---|---|
| | | | | | exp. | pred. | resi. |
| **34** | | 77 | [4] | T | 7.11 | 7.13 | -0.02 |
| **35** | | 304 | [13] | T | 6.52 | 6.49 | 0.03 |
| **36** | | 30 | [4] | P | 7.52 | 7.30 | 0.22 |
| **37** | | 424 | [7] | T | 6.37 | 6.47 | -0.10 |
| **38** | | 641 | [7] | P | 6.19 | 6.11 | 0.08 |
| **39** | | 665 | [7] | T | 6.18 | 6.14 | 0.04 |
| **40** | | 176 | [4] | P | 6.75 | 6.50 | 0.25 |
| **41** | | 3.2 | [4] | T | 8.49 | 8.66 | -0.17 |
| **42** | | 83 | [4] | T | 7.08 | 6.98 | 0.10 |
| **43** | | 462 | [4] | T | 6.34 | 6.32 | 0.02 |
| **44** | | 332 | [7] | P | 6.48 | 6.89 | -0.41 |
| **45** | | 3.2 | [7] | T | 8.49 | 8.41 | 0.08 |
| **46** | | 16.5 | [7] | T | 7.78 | 7.73 | 0.05 |
| **47** | | 374 | [7] | T | 6.43 | 6.53 | -0.10 |
| **48** | | 117 | [7] | T | 6.93 | 6.94 | -0.01 |

**Table 3** (*Continued*)
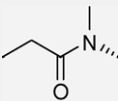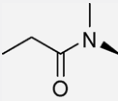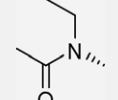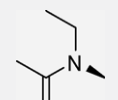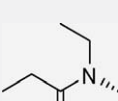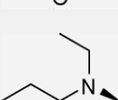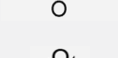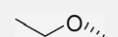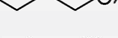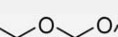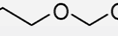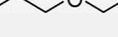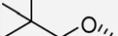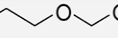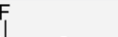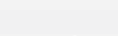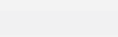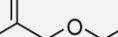
| Compound | R | $K_i$ (nM) | Ref. | Set[a] | $pK_i$[b] | | |
|---|---|---|---|---|---|---|---|
| | | | | | exp. | pred. | resi. |
| **49** | | 1.6 | [7] | T | 8.80 | 8.87 | -0.07 |
| **50** | | 6.9 | [7] | T | 8.16 | 8.16 | -0.00 |
| **51** | | 27.6 | [7] | T | 7.56 | 7.46 | 0.10 |
| **52** | | 240 | [7] | T | 6.62 | 6.65 | -0.03 |
| **53** | | 38.1 | [7] | T | 7.42 | 7.56 | -0.14 |
| **54** | | 376 | [7] | P | 6.42 | 6.77 | -0.35 |
| **55** | | 220 | [7] | P | 6.66 | 6.99 | -0.33 |
| **56** | | 7.9 | [7] | T | 8.10 | 8.16 | -0.06 |
| **57** | | 28.7 | [7] | P | 7.54 | 7.71 | -0.17 |
| **58** | | 35.8 | [4] | T | 7.45 | 7.35 | 0.10 |
| **59** | | 60.1 | [4] | P | 7.22 | 7.62 | -0.40 |
| **60** | | 0.6 | [14] | T | 9.22 | 9.27 | -0.05 |
| **61** | | 0.32 | [14] | T | 9.49 | 9.29 | 0.20 |
| **62** | | 2.2 | [14] | P | 8.66 | 8.16 | 0.50 |
| **63** | | 5.3 | [14] | T | 8.28 | 8.23 | 0.05 |
| **64** | | 1.6 | [14] | T | 8.80 | 8.86 | -0.06 |
| **65** | | 35 | [14] | T | 7.46 | 7.48 | -0.02 |
| **66** | | 1.9 | [14] | T | 8.72 | 8.86 | -0.14 |
| **67** | | 31 | [14] | P | 7.51 | 7.49 | 0.02 |
| **68** | | 141 | [14] | T | 6.85 | 6.79 | 0.06 |
| **69** | | 147 | [14] | T | 6.83 | 6.82 | 0.01 |

**Table 3** (Continued)

| Compound | R | $K_i$ (nM) | Ref. | Set[a] | pK$_i$[b] exp. | pred. | resi. |
|---|---|---|---|---|---|---|---|
| **70** | | 13 | [14] | P | 7.89 | 8.23 | -0.34 |
| **71** | | 50 | [14] | T | 7.30 | 7.44 | -0.14 |
| **72** | | 72 | [14] | T | 7.14 | 7.01 | 0.13 |
| **73** | | 75.7 | [14] | T | 7.12 | 7.13 | -0.01 |
| **74** | | 227 | [4] | T | 6.64 | 6.74 | -0.10 |

[a] T: training set; P: prediction set.
[b] exp.: experimentally determined value; pred.: predicted value; resi.: residual (experimental value – predicted value).

(Table 3). Of these, 34 compounds were chosen for the TSET with the remaining 13 compounds comprising the PSET. In this set of compounds, region focusing did not enhance the statistics of the model with the receptor-docked alignment, but did enhance the statistics of the FlexS-aligned compounds and the realignment of docked compounds. Prediction of pK$_i$ values for the FlexS alignment, however, were very poor, resulting in eleven outliers (predicted value more than 0.50 pK$_i$ units from the experimental value) out of the 48 compounds. The $q^2$ for the FlexS region-focused model was 0.502, whereas for the receptor-docked alignment (Model 2; no region focusing) $q^2 = 0.620$. The realigned dataset, after region focusing, showed poor CoMFA statistics with $q^2 = 0.320$ and resulted in six outliers out of the 47 compounds in the dataset. These alignments are shown in Fig. S2 and the statistics for the receptor-docked model (Model 2) are reported in



**Fig. 5.** Model 2 linear regression plot. Open circles and a solid line represent the training set regression. Open triangles and a dashed line show the prediction set regression.

Table 2. The linear regression plot for Model 2 is shown in Fig. 5, and the CoMFA contour maps are shown in Fig. 6.

Model 2, like Model 1, is statistically significant ($F = 395$) and predictive ($q^2 = 0.620$) and was shown to predict the external test set well (PSET $r^2 = 0.813$), with all predicted pK$_i$ values no greater than 0.50 log units from the experimental value. It should be noted that roughly 50% of the statistical outliers in the FlexS alignments (compounds **9** and **26** in Model 1 and compounds **26**, **36**, **38**, **54**, **55**, **59** and **62** in Model 2; Tables 1 and 3) were compounds that did not superimpose well in the corresponding receptor-docked alignments. This implies that these compounds might bind in an orientation that differs from that of Salvinorin A. However, the model is able to accommodate the similar but non-identical binding modes of these compounds. Each binding mode is effectively recognized by the same receptor binding site, which may be thought of as a sterically bounded three-dimensional arrangement of pharmacophoric features (H-bond acceptor and donor sites, hydrophobic regions, etc.). With respect to 3-D QSAR, the particular orientation of the ligands is relatively unimportant compared to the way in which the pharmacophoric features align with one another within the series, and in the case of structure-based 3D-QSAR, how well the pharmacophoric features of the ligands align with complementary features of the receptor. In other words, a single 3-D QSAR model (such as CoMFA) is able to effectively accommodate different orientations of structurally similar molecules. Nonetheless, when comparing members of an analogous series of compounds, one would expect to see some degree of similarity, and that is the case here.

Multiple binding modes for agonists comprising a series of structurally related compounds would seem to be less likely than for antagonists since in addition to simply binding to the receptor site, agonists must stabilize a particular receptor conformation (or conformations) recognizable by a G protein. However, it has been proposed for the β$_2$-adrenoceptor that the structurally related compounds isoproterenol and salbutamol, each with agonist activity, bind the receptor using different modes [44]. It is also possible that structurally related agonists are able to bind to and stabilize discrete intermediate conformational states of the flexible GPCR [45], with each exhibiting agonist activity. It is also possible that structurally related agonists, binding through different modes of interaction, elicit similar but distinct functional responses through functional agonism [46]; that is, different activated receptor states (that are recognized by different G proteins) may
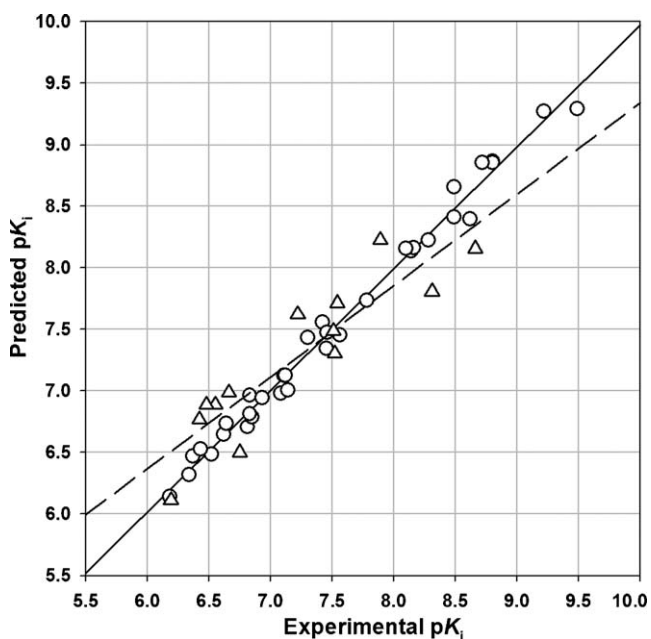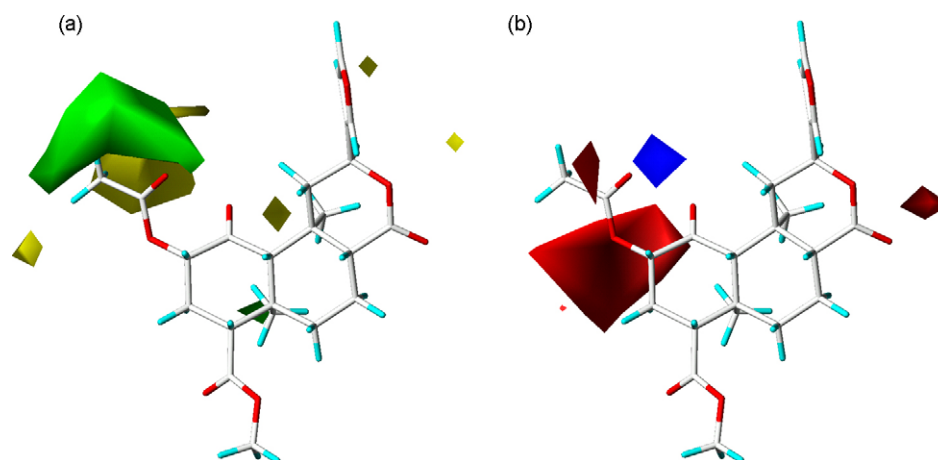
**Fig. 6.** Model 2 CoMFA maps. The color scheme is the same as in Fig. 4.

be stabilized by different agonist binding modes. Despite the conformational variability associated with functional agonism, however, there appears to be common features that are associated with an activated rhodopsin-like GPCR. These features include a movement of the intracellular portion of TM6 away from the helical bundle (i.e. opening of the "ionic lock"), with a corresponding inward movement of the extracellular part of TM6 into the ligand binding cavity, a transition that is regulated to some extent by the rotameric states of key "toggle switch" residues [47]. The proposed binding modes of the salvinorins described here each interact with the extracellular end of TM6 (I294[6.55] and E297[6.58]). These interactions may prevent the movement of the extracellular end of TM6 away from the binding site, preventing the closure of the ionic lock and serving to stabilize (not necessarily equivalent) activated forms of the KOP receptor.

The contour maps for Model 2 are qualitatively similar to those in Model 1. As in Model 1, there is a region of bulk tolerance around the C-2 ester group and a region of bulk intolerance behind it (Fig. 6a). In Fig. 6b, regions of enhanced affinity with electronegativity (red) are seen near the oxygens of the C-2 position ester group and the C-1 carbonyl. The largest area of electronegativity falls within potential H-bonding distance of H304 near the extracellular region of TM7.

It has been shown that both the methyl and carbonyl moieties of the C-2 acetoxy group contribute to the affinity of Salvinorin A for the KOP receptor [14]. Removal of the C-2 position carbonyl group (resulting in the C-2 ethyl ether) reduced the $K_i$ by 3.4-fold, and our KOP receptor-Salvinorin A interaction model suggests that the C-2 acetoxy carbonyl oxygen atom may hydrogen bond with the un-ionized acid form of E209[xI2.49]. Removal of the methyl group (resulting in the C-2 formate ester) also produced a modest drop in affinity. Mutagenesis studies have suggested that a hydrophobic interaction between the aforementioned methyl group and Y313[7.36] is present [29], and in general it seems to be important to have a hydrophobic moiety at a terminal position of the C-2 substituent for optimal ligand affinity [14]. At the same time, it has also been observed that the optimal length of the C-2 sidechain corresponds to about five heavy atoms for C-2 ethers [8], alkoxymethyl ethers [14] and esters [18], the maximum size that can be easily accommodated in the putative binding pocket.

It has been suggested that the alkoxy-oxygen of the C-2 alkoxymethyl ethers contributes to ligand binding through an H-bond interaction on the basis of the substantially reduced affinity of both the methylthiomethoxy and fluoromethoxy analogs **70** and **71**, since neither sulfur nor fluorine are good H-bond acceptors. However, the reduced affinity of these analogs may also be

explained via an alternative binding mechanism. In the proposed binding mode for the fluoromethoxy analog (**71**), the fluorine atom is situated very close to the sidechain carboxylate group of E209[xI2.49]; the close proximity of two hard electronegative atoms would thus be expected to adversely affect the ligand binding. In contrast, many of the docked poses of the alkoxymethyl ethers place the more distal alkoxy-oxygen away from any potential H-bonding functionality and in a sterically restricted region of the binding site between Y312[7.35] and Y313[7.36]. Perhaps because of steric incompatibility, the KOP receptor is predicted to recognize an alternate conformation of the methylthiomethoxy analog (**70**) in which the C-2 terminal methyl group maintains the interaction with Y313[7.36], but the remainder of the C-2 sidechain is located in a sterically less restricted region near the entrance of the binding site. The fused tricyclic salvinorin core is also shifted toward TM5 when compared with the putative binding mode of Salvinorin A (**1**); however, the placement of the furan ring is unchanged. The KOP receptor-salvinorin interaction model presented here thus suggests that increased affinity is observed with several of the alkoxymethyl ether derivatives because the oxygen atom not directly attached to the salvinorin core serves simply as a flexible linker that allows the terminal hydrophobic group to effectively interact with Y313[7.36].

It has also been observed that while monomethylation at the acetal carbon of the C-2 alkoxymethyl ethers is tolerated, dimethylation at this position can reduce the binding affinity by more than 100-fold (compare compounds **60** and **72**) [14]. Examination of the proposed binding mode of the dimethylated analog **72** shows that one of the methyl groups intersects the yellow CoMFA contour representing a region where steric bulk
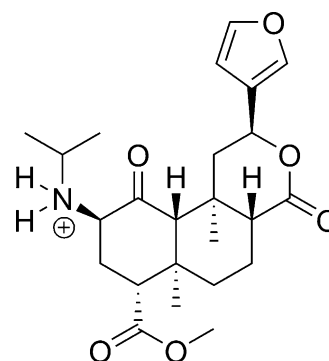


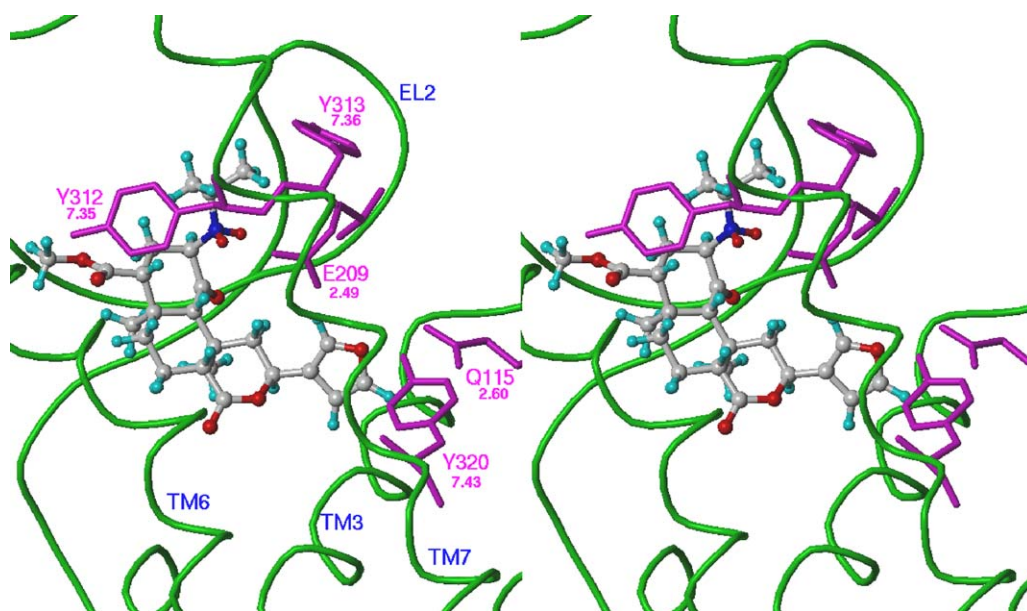**Fig. 7.** β-N-Isopropylamine analog of Salvinorin A (**75**).

**Fig. 8.** Stereo view of the β-*N*-isopropylamine analog of Salvinorin A docked in the KOP receptor.

decreases affinity (see Fig. 6). This yellow region corresponds to the backbone of the EL2 loop and the E209$^{xl2.49}$ sidechain.

Finally, it should be noted that all compounds in the analysis are predicted to have a p$K_i$ value within 0.5 log units of the experimentally determined value. This corresponds to no more than about a 3-fold difference in the $K_i$ values, which we consider to be a realistic upper bound for the experimental error associated with the $K_i$ determination. Roughly this amount of variability has been demonstrated for Salvinorin A under very similar reported experimental conditions [14,48].

### 3.5. Prediction of a C-2 amine binding mode

There is a particularly interesting region where an electropositive moiety enhances affinity (blue) near the C-2 position carbonyl oxygen atom on the β-side of the molecule (Fig. 6b). This region of electropositivity falls near E209$^{xl2.49}$, which may explain the high affinity of some amine containing analogs [7] not included in the TSET or PSET of the models described here. Docking studies of these amines reveal that the positively charged amine group likely interacts with E209$^{xl2.49}$. An example of the highest-affinity amine **75** (Fig. 7), with a reported $K_i$ of 2.3 nM [7], is shown docked in the KOP receptor (Fig. 8).

The docked position of this amine is very similar to Salvinorin A in our proposed model of the Salvinorin A–KOP receptor complex (Figs. 1 and 2). In addition to the furan oxygen having potential hydrogen bond interactions with both Q115$^{2.60}$ and Y320$^{7.43}$, the hydrogen bonding interaction between Y312$^{7.35}$ and the C-4 position methyl ester oxygen, there is a hydrophobic interaction of the methyl groups of the isopropyl substituent with the aromatic rings of both Y312$^{7.35}$ and Y313$^{7.36}$ and an ionic interaction between the positively charged nitrogen and the negatively charged sidechain of E209$^{xl2.49}$. It should also be noted that this is the β-epimer (i.e. the *R*-configuration at the C-2 position). The corresponding α-epimers (with the *S*-configuration) do not interact as well at all points mentioned here due in part to the amine being directed away from E209$^{xl2.49}$. This may explain the lower affinity of the α-isomers in this series of amine analogs, whereas the trend shown by the esters, ethers and amides is just the opposite with the α-epimer having the higher affinity. The α-*N*-isopropylamine analog has a reported $K_i$ of 17.6 nM [7].

## 4. Conclusions

In this study, two CoMFA models of Salvinorin A analogs bound to the human KOP receptor were presented whose similar contour maps coincided with the presence of complementary amino acid sidechains in the binding pocket. These models also demonstrated significant predictive ability. Model 1 analogs used [$^{125}$I]IOXY as the radioligand in the binding affinity assay while Model 2 analogs used [$^3$H]diprenorphine. The alignment that was found to produce the most statistically significant model was a receptor-docked alignment when compared with FlexS and manual realignment methods. Region focusing enhanced Model 1 but not Model 2. The contour maps revealed a region of bulk tolerance allowing for approximately a three-carbon chain from the ester carbonyl carbon. The expected enhancement of affinity with increasing electronegativity was seen around the C-2 position ester oxygens and the C-1 position carbonyl oxygen. An area of enhanced affinity corresponding to increased electropositivity on the β-side of the molecule correlated well with our postulated docked position of amine compounds in the KOP receptor and may explain the trend for the β-isomer amines to have a higher affinity than the corresponding α-isomer amines in the series. Further mutagenesis studies on the key interacting residues could be done to support or refute the postulated amine-analog binding mode.

### Acknowledgment

### Appendix A. Supplementary data

Supplementary data associated with this article can be found, in the online version, at doi:10.1016/j.jmgm.2009.12.008.

### References

[1] B.L. Roth, K. Baner, R.B. Westkaemper, D. Siebert, K.C. Rice, S. Steinberg, P. Ernsberger, R.B. Rothman, Salvinorin A: a potent naturally occurring nonnitroge-

nous κ opioid selective agonist, Proc. Natl. Acad. Sci. U.S.A. 99 (2002) 11934–11939.

[2] A. Ortega, J.F. Blount, P.S. Manchand, Salvinorin, a New *trans*-Neoclerodane Diterpene from *Salvia divinorum* (Labiatae), J. Chem. Soc. Perkins Trans. 1 (1982) 2505–2508.

[3] L.J. Valdes III, W.M. Butler, G.M. Hatfield, A.G. Paul, M. Koreeda, Divinorin A, a Psychotropic Terpenoid, and Divinorin B from the Hallucinogenic Mexican Mint *Salvia Divinorum*, J. Org. Chem. 49 (1984) 4716–4720.

[4] C. Beguin, W.A. Carlezon Jr., B.M. Cohen, M. He, D.Y.-W. Lee, M.R. Richards, Salvinorin derivatives and uses thereof, WO 2005/089745, 2005.

[5] C. Beguin, W.A. Carlezon Jr., B.M. Cohen, M. He, D.Y.-W. Lee, M.R. Richards, L.-Y. Liu-Chen, Salvinorin derivatives and uses thereof, US2007/0213394, 2007.

[6] C. Béguin, D.N. Potter, J.A. DiNieri, T.A. Munro, M.R. Richards, T.A. Paine, L. Berry, Z. Zhao, B.L. Roth, W. Xu, L.-Y. Liu-Chen, W.A. Carlezon Jr., B.M. Cohen, *N*-Methylacetamide analog of Salvinorin A: a highly potent and selective κ-opioid receptor agonist with oral efficacy, J. Pharmacol. Exp. Ther. 324 (2008) 188–195.

[7] C. Béguin, M.R. Richards, J.-G. Li, Y. Wang, W. Xu, L.-Y. Liu-Chen, W.A. Carlezon Jr., B.M. Cohen, Synthesis and in vitro evaluation of Salvinorin A analogues: effect of configuration at C(2) and substitution at C(18), Bioorg. Med. Chem. Lett. 16 (2006) 4679–4685.

[8] C. Béguin, M.R. Richards, Y. Wang, Y. Chen, L.-Y. Liu-Chen, Z. Ma, D.Y.W. Lee, W.A. Carlezon Jr., B.M. Cohen, Synthesis and in vitro pharmacological evaluation of Salvinorin A analogues modified at C(2), Bioorg. Med. Chem. Lett. 15 (2005) 2761–2765.

[9] R.V. Bikbulatov, F. Yan, B.L. Roth, J.K. Zjawiony, Convenient synthesis and in vitro pharmacological activity of 2-thioanalogs of Salvinorins A and B, Bioorg. Med. Chem. Lett. 17 (2007) 2229–2232.

[10] C. Chavkin, S. Sud, W. Jin, J. Stewart, J.K. Zjawiony, D. Siebert, B.A. Toth, S.J. Hufeisen, B.L. Roth, Salvinorin A, an active component of the hallucinogenic sage *Salvia Divinorum* is a highly efficacious κ-opioid receptor agonist: structural and functional considerations, J. Pharmacol. Exp. Ther. 308 (2004) 1197–1203.

[11] W.W. Harding, K. Tidgewell, N. Byrd, H. Cobb, C.M. Dersch, E.R. Butelman, R.B. Rothman, T.E. Prisinzano, Neoclerodane diterpenes as a novel scaffold for μ opioid receptor ligands, J. Med. Chem. 48 (2005) 4765–4771.

[12] D.Y.W. Lee, V.V.R. Karnati, M. He, L.-Y. Liu-Chen, L. Kondaveti, Z. Ma, Y. Wang, Y. Chen, C. Beguin, W.A. Carlezon Jr., B. Cohen, Synthesis and in vitro pharmacological studies of new C(2) modified Salvinorin A analogues, Bioorg. Med. Chem. Lett. 15 (2005) 3744–3747.

[13] T.A. Munro, K.K. Duncan, R.J. Staples, W. Xu, L.-Y. Liu-Chen, C. Béguin, W.A. Carlezon Jr., B.M. Cohen, 8-*epi*-Salvinorin B: crystal structure and affinity at the κ opioid receptor Beilstein, J. Org. Chem. 3 (2007) 1.

[14] T.A. Munro, K.K. Duncan, W. Xu, Y. Wang, L.-Y. Liu-Chen, W.A. Carlezon Jr., B.M. Cohen, C. Béguin, Standard protecting groups create potent and selective κ opioids: Salvinorin B alkoxymethyl ethers, Bioorg. Med. Chem. 16 (2008) 1279–1286.

[15] T. Prisinzano, Opioid Receptor Ligands and Methods for their Preparation, US2006/0058264, 2006.

[16] D.J. Stewart, H. Fahmy, B.L. Roth, F. Yan, J.K. Zjawiony, Bioisosteric modification of Salvinorin A, a potent and selective kappa-opioid receptor agonist, Arzneimittelforschung 56 (2006) 269–275.

[17] K Tidgewell, C.E. Groer, W.W. Harding, A. Lozama, M. Schmidt, A. Marquam, J. Heimstra, J.S. Partilla, C.M. Dersch, R.B. Rothman, L.M. Bohn, T.E. Prisinzano, Herkinorin analogues with differential β-arrestin-2 interactions, J. Med. Chem. 51 (2008) 2421–2431.

[18] K. Tidgewell, W.W. Harding, A. Lozama, H. Cobb, K. Shah, P. Kannan, C.M. Dersch, D. Parrish, J.R. Deschamps, R.B. Rothman, T.E. Prisinzano, Synthesis of Salvinorin A analogs as opioid receptor probes, J. Nat. Prod. 69 (2006) 914–918.

[19] J.K. Zjawiony, H. Fahmy, D.J. Stewart, B.L. Roth, Agents with Selective Kappa-Opioid Receptor Affinity, WO 2006/012643, 2006.

[20] D.Y.W. Lee, M. He, L. Kondaveti, L.-Y. Liu-Chen, Z. Ma, Y. Wang, Y. Chen, J.-G. Li, C. Beguin, W.A. Carlezon Jr., B. Cohen, Synthesis and in vitro pharmacological studies of C(4) modified Salvinorin A analogues, Bioorg. Med. Chem. Lett. 15 (2005) 4169–4173.

[21] D.Y.W. Lee, M. He, L.-Y. Liu-Chen, Y. Wang, J.-G. Li, W. Xu, Z. Ma, W.A. Carlezon Jr., B. Cohen, Synthesis and in vitro pharmacological studies of new C(4) modified Salvinorin A analogues, Bioorg. Med. Chem. Lett. 16 (2006) 5498–5502.

[22] W.W. Harding, M. Schmidt, K. Tidgewell, P. Kannan, K.G. Holden, C.M. Dersch, R.B. Rothman, T.E. Prisinzano, Synthetic studies of neoclerodane diterpenes from *Salvia divinorum*: selective modification of the furan ring, Bioorg. Med. Chem. Lett. 16 (2006) 3170–3174.

[23] D.S. Simpson, P.L. Katavic, A. Lozama, W.W. Harding, D. Parrish, J.R. Deschamps, C.M. Dersch, J.S. Partilla, R.B. Rothman, H. Navarro, T.E. Prisinzano, Synthetic studies of neoclerodane diterpenes from *Salvia divinorum*: preparation and opioid receptor activity of salvinicin analogues, J. Med. Chem. 50 (2007) 3596–3603.

[24] F. Yan, P.D. Mosier, R.B. Westkaemper, B.L. Roth, Gα-subunits differentially alter the conformation and agonist affinity of κ-opioid receptors, Biochemistry 47 (2008) 1567–1578.

[25] N. Singh, G. Cheve, D.M. Ferguson, C.R. McCurdy, A combined ligand-based and target-based drug design approach for g-protein coupled receptors: application to

Salvinorin A, a selective kappa opioid receptor agonist, J. Comput. Aided Mol. Des. 20 (2006) 471–493.

[26] D. Pandit, W.W. Harding, K. Tidgewell, M. Schmidt, A. Lozama, C.M. Dersch, W.J. Skawinski, R.B. Rothman, T.E. Prisinzano, C.A. Venanzi, 233rd ACS National Meeting, Chicago, IL, 2006.

[27] R.D. Cramer III, D.E. Patterson, J.D. Bunce, Comparative molecular field analysis (CoMFA). 1: effect of shape on binding of steroids to carrier proteins, J. Am. Chem. Soc. 110 (1988) 5959–5967.

[28] T. Vortherms, P.D. Mosier, R.B. Westkaemper, B.L. Roth, Differential helical orientations among related G protein-coupled receptors provide a novel mechanism for selectivity: studies with Salvinorin A and the κ-opioid receptor, J. Biol. Chem. 282 (2007) 3146–3156.

[29] F. Yan, P.D. Mosier, R.B. Westkaemper, J. Stewart, J.K. Zjawiony, T. Vortherms, D.J. Sheffler, B.L. Roth, Identification of the molecular mechanisms by which the diterpenoid Salvinorin A binds to κ-opioid receptors, Biochemistry 44 (2005) 8643–8651.

[30] C. Lemmen, T. Lengauer, G. Klebe, FlexS: A method for fast flexible ligand superpositions, J. Med. Chem. 41 (1998) 4502–4520.

[31] S.A. Hjorth, K. Thirstrup, T.W. Schwartz, Radioligand-dependent discrepancy in agonist affinities enhanced by mutations in the κ-opioid receptor, Mol. Pharmacol. 50 (1996) 977–984.

[32] M.M. Rosenkilde, M. Cahir, U. Gether, S.A. Hjorth, T.W. Schwartz, Mutations along Transmembrane Segment II of the NK-1 receptor affect substance P competition with non-peptide antagonists but not substance P binding, J. Biol. Chem. 269 (1994) 28160–28164.

[33] P.Y. Law, T.M. McGinn, M.J. Wick, L.J. Erikson, C. Evans, H.H. Loh, Analysis of *Delta*-opioid receptor activities stably expressed in CHO cell lines: function of receptor density? J. Pharmacol. Exp. Ther. 271 (1994) 1686–1694.

[34] J.A. Ballesteros, H. Weinstein, Integrated methods for the construction of three-dimensional models and computational probing of structure–function relationships in G-protein coupled receptors, Methods Neurosci. 25 (1995) 366–428.

[35] H. Xhaard, T. Nyrönen, V.-V. Rantanen, J.O. Ruuskanen, J. Laurila, T. Salminen, M. Scheinin, M.S. Johnson, Model structures of α-2 adrenoreceptors in complex with automatically docked antagonist ligands raise the possibility of interactions dissimilar from agonist ligands, J. Struct. Biol. 150 (2005) 126–143.

[36] S.J. Cho, A. Tropsha, Cross-validated $R^2$-guided region selection for comparative molecular field analysis: a simple method to achieve consistent results, J. Med. Chem. 38 (1995) 1060–1066.

[37] B.E. Kane, M.J. Nieto, C.R. McCurdy, D.M. Ferguson, A unique binding epitope for Salvinorin A, a non-nitrogenous kappa opioid receptor agonist, FEBS J. 273 (2006) 1966–1974.

[38] B.E. Kane, C.R. McCurdy, D.M. Ferguson, Toward a structure-based model of Salvinorin A recognition of the κ-opioid receptor, J. Med. Chem. 51 (2008) 1824–1830.

[39] F. Yan, R.V. Bikbulatov, V. Mocanu, N. Dicheva, C.E. Parker, W.C. Wetsel, P.D. Mosier, R.B. Westkaemper, J.A. Allen, J.K. Zjawiony, B.L. Roth, Structure-based design, synthesis, and biochemical and pharmacological characterization of novel Salvinorin A analogues as active state probes of the κ-opioid receptor, Biochemistry 48 (2009) 6898–6908.

[40] D. Salom, D.T. Lodowski, R.E. Stenkamp, I. Le Trong, M. Golczak, B. Jastrzebska, T. Harris, J.A. Ballesteros, K. Palczewski, Crystal structure of a photoactivated deprotonated intermediate of rhodopsin, Proc. Natl. Acad. Sci. U. S. A. 103 (2006) 16123–16128.

[41] C. de Graaf, N. Foata, O. Engkvist, D. Rognan, Molecular modeling of the second extracellular loop of G-protein coupled receptors and its implication on structure-based virtual screening, Proteins 71 (2008) 599–620.

[42] J.C. Mobarec, R. Sanchez, M. Filizola, Modern homology modeling of G-protein coupled receptors: which structural template to use? J. Med. Chem. 52 (2009) 5209–5216.

[43] R.D. Clark, A ligand's-eye view of protein binding, J. Comput. Aided Mol. Des. 22 (2008) 507–521.

[44] G. Swaminath, X. Deupi, T.W. Lee, W. Zhu, F.S. Thain, T.S. Kobilka, B.K. Koblika, Probing the β₂ adrenoceptor binding site with catechol reveals differences in binding and activation by agonists and partial agonists, J. Biol. Chem. 280 (2005) 22165–22171.

[45] G. Swaminath, Y. Xiang, T.W. Lee, J. Steenhuis, C. Parnot, B. Kobilka, Sequential binding of agonists to the β₂ adrenoceptor: kinetic evidence for intermediate conformational states, J. Biol. Chem. 279 (2004) 686–691.

[46] T. Kenakin, Functional selectivity through protean and biased agonism: who steers the ship? Mol. Pharmacol. 72 (2007) 1393–1401.

[47] R. Nygaard, T.M. Frimurer, B. Holst, M.M. Rosenkilde, T.W. Schwartz, Ligand binding and micro-switches in 7TM receptor structures, Trends Pharmacol. Sci. 30 (2009) 249–259.

[48] D.Y.W. Lee, Z. Ma, L.-Y. Liu-Chen, Y. Wang, Y. Chen, W.A. Carlezon Jr., B. Cohen, New neoclerodane diterpenoids isolated from the leaves of *Salvia divinorum* and their binding affinities for human κ opioid receptors, Bioorg. Med. Chem. 13 (2005) 5635–5639.